

Study of Rodlike Homopolypeptides by Gel Permeation Chromatography with Light Scattering Detection: Validity of Universal Calibration and Stiffness Assessment

Elena Temyanko, Paul S. Russo,* and Holly Ricks

Department of Chemistry and Macromolecular Studies Group, Louisiana State University, Baton Rouge, Louisiana 70803-1804

Received August 1, 2000; Revised Manuscript Received November 7, 2000

ABSTRACT: Gel permeation chromatography with simultaneous light scattering measurements has been performed on poly(γ -benzyl- α -L-glutamate) and poly(γ -stearyl- α -L-glutamate) in *N,N*-dimethylformamide and tetrahydrofuran, respectively. Intrinsic viscosities were computed by combining the measured molecular weights with literature values for the Mark–Houwink parameters. The product of intrinsic viscosity and molecular weight for the rodlike polymers, when plotted against elution volume, overlaid the results for polystyrene, a random coil. In the excluded-volume limit, similar convergence was observed for the second virial coefficient of osmotic pressure as a function of polymer number density. In the case of poly(γ -benzyl- α -L-glutamate) the radius of gyration increased linearly with mass up to at least $M = 100\,000$, corresponding to a contour length of 70 nm. Slight deviations from linear behavior at higher mass suggest a persistence length in the upper range of literature values based on measurements that did not have the advantage of chromatographic separation.

Introduction

Gel permeation chromatography (GPC) is still the most popular, rapid, and reliable way to determine the molecular weight and distribution of synthetic polymers. The separation of macromolecules by size is effected by an inert stationary phase such as agarose, cross-linked dextran, silica, or vinyl polymer gels. The procedure may be called size exclusion chromatography by synthetic chemists or gel filtration chromatography by biochemists. Early experiments were time-consuming and suffered from many limitations. Today the separation may require just minutes. Annoying column and equipment failures still occur, but less frequently. High-performance column packings, improved detector sensitivity, and optimization of the interdetector volumes may reduce the analysis time even further in the future. A major drawback of early experiments was the need to calibrate the column with various standards of narrow polydispersity and the same chemical composition as the sample. When this was not possible, the GPC molecular weight was only relative to whatever standards had been chosen during calibration. In 1967 Benoit and co-workers introduced universal calibration.^{1–3} They found that polymers having different chemical identities fell on the same graph of $\log([\eta]M)$ versus elution volume, V_e , where $[\eta]$ is the intrinsic viscosity. This enabled a rational correction procedure to be applied in the common case that the polymer to be analyzed was not the same type of polymer used for calibrating the column.

The validity of universal calibration is questionable. The underlying idea is that the product $[\eta]M$ represents the hydrodynamic volume of a macromolecule and, therefore, its ability to penetrate the porous particles comprising the stationary phase.^{4,5} Molecules with similar $[\eta]M$ should elute at the same time. For rapidly rotating, spherically symmetrical polymers such as

linear random coils and most branched macromolecules, this seems reasonable; however, several authors report failures.^{6–10} One purpose of the present work is to test the validity of universal calibration using rodlike polymers, which are hydrodynamically distinct from random coils or branched polymers. To this old strategy³ we add in-line light scattering detection (GPC/LS) and two homopolypeptides, the venerable poly(γ -benzyl- α -L-glutamate) (PBLG) and the somewhat newer poly(γ -stearyl- α -L-glutamate) (PSLG), in different solvents. These polymers display a very stiff α -helical conformation in appropriate solvents such as *N,N*-dimethylformamide (DMF) for PBLG and tetrahydrofuran (THF) for PSLG. Radially extended side chains surround a cylindrical backbone to provide good solubility. A second purpose of the present work is to explore the stiffness of these helical polypeptides, a difficult task since they are not commonly available in lengths that exhibit much bending.

Background and Strategy

In the Mark–Houwink relation

$$[\eta] = KM^a \quad (1)$$

the parameters K and a depend on the polymer, solvent, and temperature and slightly on the range of molecular weights.^{1,2} By the universal calibration hypothesis, at a given value of V_e , the polymer to be analyzed (A) and the polymer standard (S) share the same product, $[\eta]M$:

$$[\eta]_A M_A = [\eta]_S M_S \quad (2)$$

or

$$K_A M_A^{a_A+1} = K_S M_S^{a_S+1} \quad (3)$$

If the Mark–Houwink values for polymers A and S are both known, eq 3 can be solved for M_A under the

* Communicating author.

Table 1. GPC/LS Parameters for PS in THF

M_w		M_w/M_n
vendor specified	this work ^a	this work ^b
3 105	N/A	1.14
6 207	N/A	1.03
10 300	10 250	1.03
43 900	45 900	1.01
102 000	105 800	1.02
212 000	240 900	1.01
170 000	174 700	1.01
422 000	483 900	1.02
929 000	935 900	1.01
1 600 000	1 639 000	1.16
1 971 000	2 226 000	1.03
2 145 000	2 171 000	1.1

^a GPC/LS. ^b Sensitive to baseline and peak selection.

Table 2. PSLG Molecular Weights

M_w	M_w/M_n	M_w	M_w/M_n
13 370	2.04	138 400	1.02
17 570	2.04	150 800	1.24
51 080	1.04	176 000	1.13
67 700	1.02	249 000	1.03
93 090	1.26		

universal hypothesis. If an in-line viscosity detector (see, for example, refs 11 and 12) is used, then one need not even know the Mark–Houwink values for the analyte; eq 2 can be solved directly for M_A . These very important simplifications rely on the validity of the universal calibration hypothesis.

One can design several strategies for testing universal calibration. Triple detector measurements of polymers having a very wide distribution might seem the most elegant. In this powerful method, the molecular weight is available from the light scattering and concentration detectors, while the latter combines with a viscosity detector to provide $[\eta]$. The main drawback is inter-detector alignment. As the polymer flows first to one detector and then to the next, it is necessary to compare the raw signals after separation by an appropriate time delay. The different response, flow characteristics, and band broadening of the three detectors make this difficult.¹³ Also, even with broadly polydisperse samples (for the polypeptides under consideration, this would require mixtures), critical data tend to lie in the “wings”, i.e., near the baseline, where errors can corrupt the results. For these reasons, it is actually not trivial to establish Mark–Houwink and other scaling exponents spanning a decade or more in molecular weight using triple detector techniques. The scaling exponents obtained laboriously from the older batch studies of well-fractionated polymers may prove more accurate.

Instead of a triple detector approach, we combine Mark–Houwink data from classical batch studies on polypeptides and polystyrene with GPC/LS data for molar mass determination. This eliminates one detector. Once M_w is measured from GPC/LS, we simply compute $[\eta]$ using literature values for the Mark–Houwink parameters. The product of M_w and $[\eta]$ is plotted against V_e , and independence of the results on polymer architecture is assessed. This strategy is appealing because both polystyrenes and most polypeptides have reasonably low polydispersities as a result of their synthetic pathways (see Tables 1–3) and because both have been studied extensively over a range of M . Some of our classically initiated polypeptides have polydispersity index values that are the equal of the polymers produced

Table 3. PBLG Molecular Weights

M_w	M_w/M_n	M_w	M_w/M_n
10 700	1.23	71 000	1.12
13 700	1.27	86 000	1.02
18 500	1.23	96 000	1.05
30 000	1.07	265 000	1.18
46 000	1.05	327 500	1.04

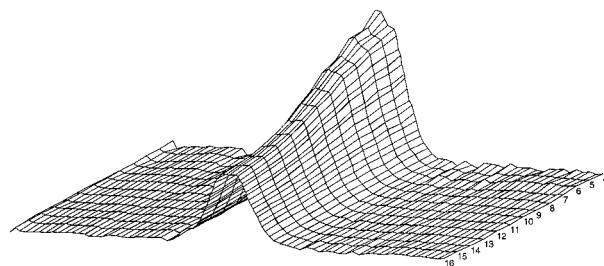


Figure 1. Elution profile for PBLG in DMF for 13 scattering angles, approximately 20°–140°, with lower numbers corresponding to lower angles.

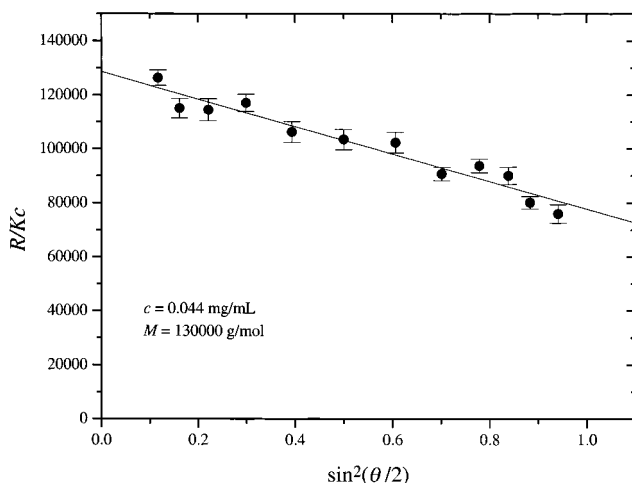


Figure 2. Scattering intensity envelope for a single slice of one chromatogram.

by newer initiation strategies.^{14–16} Certain preparations must be excluded from this analysis because their dispersion is too high, but these samples, and mixtures of them, prove useful for estimating chain stiffness. The Mark–Houwink equations used, for $[\eta]$ in mL g^{−1}, are

$$[\eta] = 0.011 M_w^{0.725} \quad \text{for PS}^{17} \quad (4)$$

$$[\eta] = 1.26 \times 10^{-5} M_w^{1.29} \quad \text{for PSLG}^{18} \quad (5)$$

$$[\eta] = 1.58 \times 10^{-5} M_w^{1.35} \quad \text{for PBLG}^{19} \quad (6)$$

The Mark–Houwink values for PSLG were obtained¹⁸ using samples whose polydispersities were not well characterized at the time, although dynamic light scattering and other considerations did suggest reasonable uniformity. Table 2 shows that most PSLG samples are indeed quite narrowly distributed. The Mark–Houwink parameters for PBLG result from a reanalysis of data by Fujita et al.²⁰ and Doty et al.²¹ and newer data from this lab,¹⁹ all in helicogenic solvents. We take this opportunity to correct errors of presentation made in a previous paper from this laboratory, ref 19. In Figure 2 of ref 19 the symbols for the data of Doty and Fujita were mistakenly swapped. Thus, the claim of agreement with the Mark–Houwink parameters of Doty

et al. is incorrect; the new Mark–Houwink results in ref 19 agree better with those of Fujita et al. Also, in the discussion of Figure 2 of ref 19 numbers like 6.8 are not the Mark–Houwink K value. Rather, $\log K = -6.8$ for $[\eta]$ in dL/g; equivalently, $\log K = -4.8$ for $[\eta]$ in mL g⁻¹. For all the polymers, we have used simple linear Mark–Houwink relationships, even though the collected data on PBLG in helicogenic solvents suggest that minor curvature is present; see Figure 2 of ref 19.

Experimental Section

The synthesis of the PBLG and PSLG was previously described.^{18,22,23} Additionally, some PBLG samples were purchased from Sigma. Polystyrene standards were obtained from Scientific Polymer Products, Inc., and from Toyo-Soda. HPLC grade solvents were used as received. Care was taken to keep the highly hygroscopic DMF dry. The GPC system consisted of a Waters 590 pump, a Waters sample injector, a Wyatt DAWN DSP multiangle light scattering detector operating at 632.8 nm, and a Waters 410 differential refractive index detector. The column set included a Phenomenex 7.8 × 50 mm guard column plus tandem Phenomenex Phenogel 10 MXM and 10⁵ Å columns (7.8 × 300 mm, 10 μm bead size, suitable for polystyrene molar masses of 5000–1 000 000). The mobile phase (THF for PS and PSLG, DMF for PBLG) was kept under nitrogen to prevent moisture contamination, degassed by sparging with dried helium for several hours before experiment, and filtered through a 0.2 μm Whatman filter prior to use. The temperature was 25 °C, and the flow rate was 0.90 mL min⁻¹. Sample concentration was 0.5–6 mg mL⁻¹, depending on molar mass, and the injection volume was 100 μL. The differential refractometer was calibrated by measuring the voltage output for a series of Dow Polystyrene 1683 solutions in THF using as the specific refractive index increment $dn/dc = 0.185$ mL g⁻¹. The same dn/dc value was used to determine the mass concentrations of PS standards for GPC/LS experiments in THF. Other dn/dc values used were 0.080 mL g⁻¹ for PSLG in THF¹⁸ and 0.118 mL g⁻¹ for PBLG in DMF²⁴ (respective dn/dc uncertainties: ±0.002 and ±0.004 mL g⁻¹). For PS in DMF dn/dc was taken as 0.1615 mL g⁻¹, which is within about ±0.001 mL g⁻¹ of the long-wavelength data of Mächtle and Fischer, as listed in the text by Huglin.²⁵ It was assumed that dn/dc did not vary with M . All polymers were completely dissolved after 3–4 h with occasional stirring. The columns were calibrated with 12 PS standards ($M = 3000$ – $2\,100\,000$) in THF. Elution volumes of PS were very similar in DMF, despite expressed concerns about nonsize separations for PS in DMF (see ref 26 and references therein). Perhaps this represents progress in stationary phases or the care that was taken in the present study to maintain the DMF in a dry condition.

The DAWN model DSP multiangle light scattering detector can measure scattered light intensities at up to 18 different angles. The number of usable angles depends on solvent refractive index. While analyzing high-molecular-weight polymers, data obtained at some usable angles may be disregarded in order to obtain good linearization and accurate radii. Light scattering intensity chromatograms from 13 scattering angles (23° < θ < 143°) for PBLG ($M_w = 265\,000$) appear in Figure 1.

The evaluation of molecular weights and sizes was accomplished by ASTRA software (version 4.5 or 4.7) using the so-called “Debye” fit method, based on the following equation:

$$R(\theta)/Kc = MP(\theta) - 2A_2cM^2P^2(\theta) \quad (7)$$

where $R(\theta)$ is the excess Rayleigh factor, θ is the scattering angle, $K = 4\pi^2 n_0^2 (dn/dc)^2 \lambda_0^{-4} N_a^{-1}$ is an optical constant, c is the mass/volume concentration of the solute, n_0 is the refractive index of the solvent at the incident radiation wavelength, λ_0 , N_a is Avogadro's number, and A_2 is the osmotic second virial coefficient. The form factor, $P(\theta)$, is given at low scattering angles by $1 - q^2 R_g^2/3$ where R_g is the radius of gyration and q

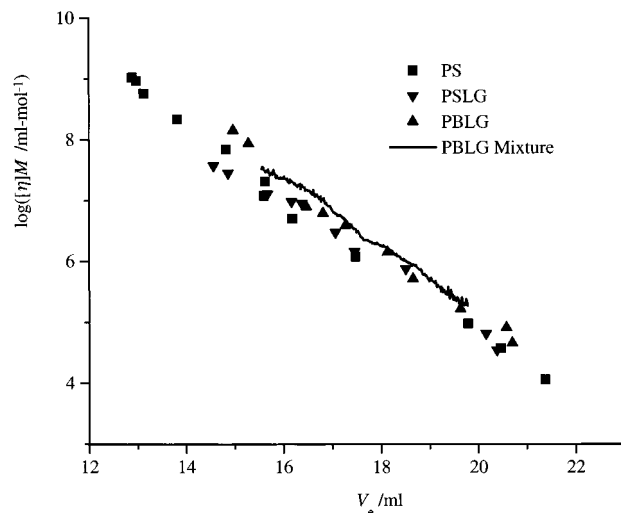


Figure 3. Universal calibration plots for PS, PSLG, and PBLG. Also shown is a trace derived from a single GPC/LS run.

$= 4\pi n \sin(\theta/2)/\lambda_0$, with n the refractive index. A sample plot for PBLG-265000 appears in Figure 2. The intercept at zero angle, R_0/Kc , and the slope at zero angle, m_0 , were found in order to calculate M and R_g from second or third degree polynomial fits to the data using following equations:

$$M = \frac{1 - \sqrt{1 - 8A_2c \frac{R_0}{Kc}}}{4A_2c} \quad (8a)$$

$$R_g^2 = \frac{-3m_0\lambda^2}{16\pi^2 M(1 - 4A_2M)} \quad (8b)$$

where λ is the light wavelength in the solution. A molecular weight invariant value for A_2 , chosen to represent the molecular weight range being studied, is often used. The low concentrations of GPC/LS normally support this assumption for the purpose of obtaining M and R_g , but we shall later be interested in the M dependence of A_2 . Where rodlike polymers are concerned, the molecular weight invariance is an even better assumption.²⁷

Results and Discussion

Universal Calibration. The measured molecular weights for PS in THF agree well with those specified by the vendor, as shown in Table 1 where polydispersity parameters, M_w/M_n , also appear. The M_w/M_n parameters measured by GPC/LS are somewhat smaller than those claimed by the vendor; perhaps this is because the polydispersity index in GPC/LS is sensitive to baseline and peak selection. Measured parameters for PSLG and PBLG appear in Tables 2 and 3, respectively. Figure 3 shows combined universal calibration curves for PS, PSLG, and PBLG. Casual inspection suggests no significant differences. When 98% confidence limits are drawn, the data sets actually are just barely distinguishable at some elution volumes; still, the universal hypothesis seems valid for almost any practical purpose. Also shown is a continuous curve constructed from a single GPC/LS measurement of a mixture of PBLG samples. It lies completely within the 98% confidence limits of a linear fit to the individual PBLG data points.

The product $[\eta]M$ represents one estimate of the polymer volume, involving both hydrodynamic ($[\eta]$) and

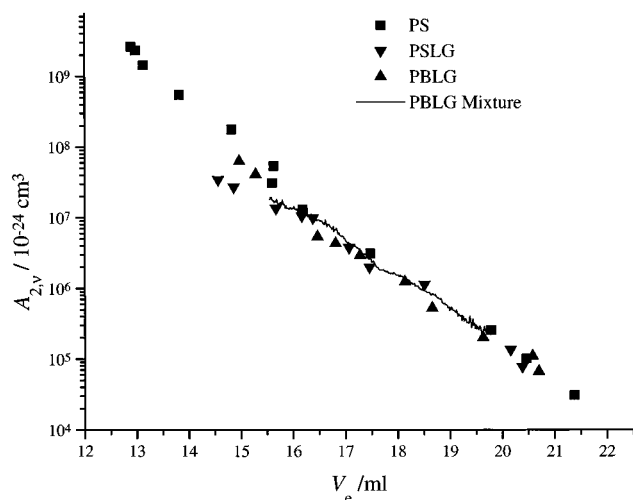


Figure 4. Osmotic second virial coefficient (for polymer content specified as number density) is another successful descriptor of elution volume. The virial coefficient is derived from an equation valid in the excluded-volume limit and does not reflect attractive interactions that, when present, quickly lead to phase separation for stiff polymers.

thermodynamic (M) parameters. Another estimate of the polymer volume can be obtained from the osmotic second virial coefficient *in the excluded-volume limit*. In this limit, attractions are ignored, as are electrostatic repulsions. Neither factor is too worrisome for uncharged polymers in good solvents, but the immediately following considerations should not be extended to Θ conditions, poor solvent conditions, or polyelectrolytes. Although it is customary to express concentrations as weight/volume, more physical insight is available when number density units (e.g., ν = solute molecules/mL) are used. In those units, the osmotic second virial coefficient, $A_{2,\nu}$, is defined through the relation

$$\pi = \nu kT(1 + \nu A_{2,\nu} + \dots) \quad (9)$$

with π the osmotic pressure, k Boltzmann's constant, and T the Kelvin temperature. The relationship between $A_{2,\nu}$ and the usual virial coefficient, A_2 , for concentration expressed in g mL^{-1} is

$$A_{2,\nu} = M^2 A_2 / N_a \quad (10)$$

For rigid rods, $A_{2,\nu}$ is the volume swept out as the rod rotates end over end about its midpoint:²⁸

$$A_{2,\nu} = dL^2/4 \quad (11)$$

In this expression, d is the diameter, 1.6 nm for PBLG and 3.6 nm for PSLG,^{18,24} and $L = \delta M/M_0$ is the contour length, where δ is the projection along the helix axis per monomer repeat unit, 0.15 nm for the α -helix. The monomer mass, M_0 , is 219 for PBLG and 382 for PSLG. Thus, $A_{2,\nu}$ for the rodlike polymers is easily computed from M . For polystyrene, $A_{2,\nu}$ can be computed from eq 10 and the experimental results for A_2 in THF.²⁹

$$A_2 \text{ (in mL mol g}^{-2}\text{)} = 0.0194M^{-0.286} \quad (12)$$

Figure 4 shows that $A_{2,\nu}$ values for PS, PSLG, and PBLG are all similar at a given elution volume, except for early eluting PSLG samples. The convergence in these good solvents is slightly better than for the product $[\eta]M$.

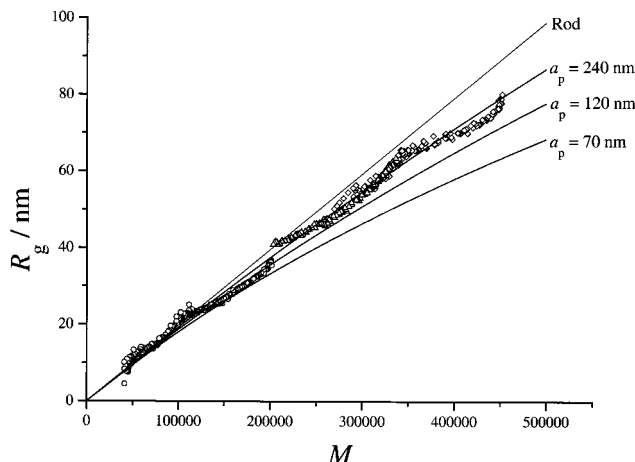


Figure 5. Radius of gyration increases linearly with molecular weight for PBLG in DMF. The varied symbols correspond to different samples, measured separately.

Other geometric parameters, such as axial ratio of the rods or the volume L^3 , do not successfully scale the data.

Chain Stiffness. A plot of R_g vs M appears in Figure 5. It is constructed from separate measurements of three different samples, including one that is already a mixture of separate polymers. In principle, it would be better to inject one very broad sample. Due to instrument sensitivity limitations, this could require overloading of the column to ensure detectable signals at the peak extremities. Despite some wrinkles, the data from our three separate measurements join to give a consistent trend that is approximately linear, as expected for a rodlike polymer. The upper straight line represents the radius of gyration calculated in the thin rod limit as

$$R_{g,\text{calc}} = \frac{L}{\sqrt{12}} = \frac{\delta M/M_0}{\sqrt{12}} \quad (13)$$

The oscillations of the data about the trend line are probably an artifact, reflecting that the samples are composed of narrowly distributed polymers and their mixtures. The sharp peaks of such samples exacerbate even minor interdetector misalignments. This wobbling hampers efforts to determine stiffness parameters precisely, but important information can yet be extracted. There are certainly no significant deviations from the rod limit up to $M = 100\,000$ ($L = 70$ nm). The apparent sudden change of slope at slightly higher mass is probably an artifact, but significant deviations from linearity are evident by $M = 300\,000$ ($L = 210$ nm). One may calculate R_g for wormlike chains of persistence length a_p using the equation^{30,31}

$$R_g^2 = \frac{La_p}{3} - a_p^2 + \frac{2a_p^3}{L} \left[1 - \frac{a_p}{L}(1 - e^{-L/a_p}) \right] \quad (14)$$

Curves are shown in Figure 5 for $a_p = 240$, 120, and 70 nm. These values span the range of most previous estimates of the persistence length of PBLG in good, helicogenic solvents (see, for examples, refs 32–35 and references therein). The present results favor a persistence length on the higher side of the reported range, perhaps because the effects of polydispersity³⁵ have been vanquished; still, a truly reliable value for the persistence length of PBLG remains out of reach. Figure 5 is plotted on a linear scale; log–log plots constructed for

the several samples of PBLG in DMF gave an apparent Flory scaling parameter ν_F (as in $R_g \sim M^{\nu_F}$) of 0.85 ± 0.06 . This compares favorably to the corresponding exponent from dynamic light scattering, a hydrodynamic method, on narrowly distributed samples, which is 0.78 ± 0.05 .^{35,36} Either exponent reflects not only the intrinsic chain stiffness but also the range of mass studied, which is limited compared to studies of typical random coils.

GPC experiments on PBLG were previously performed by Grubisic et al.³ in DMF and by Dawkins and Hemming²⁶ in dimethylacetamide at 80 °C. These solvent conditions were intended to prevent association of PBLG, which is highly sensitive to moisture.³⁷ We used pure DMF instead, taking care to avoid water contamination. An aggregation test for PBLG in DMF at 25 °C using analytical ultracentrifugation did not show any sign of association for narrow molecular weight samples; however, peaks corresponding to aggregates were occasionally observed in GPC/LS. Such data have been excluded in the above analysis, and it is believed the results for PBLG in DMF reflect single-molecule, good-solvent behavior. For PSLG in THF, the plot analogous to Figure 5 was much noisier due to the low inherent scattering of this system ($dn/dc = 0.080 \text{ mL g}^{-1}$). Meaningful persistence lengths and scaling exponents for PSLG in THF could not be obtained with the present equipment and polymer samples.

Conclusion

Universal calibration appears valid for flexurally stiff polypeptides over the range of molecular weights normally available. This may prove a useful result for the characterization of a wide variety of homopolypeptides and copolypeptides that can be prepared using novel metal complex initiation schemes.^{14–16} It remains difficult to estimate persistence lengths of the synthetic homopolypeptides, but the removal of residual polydispersity does appear to favor a very high value for the persistence length of PBLG. The assumption of a rodlike shape for the polypeptides results in osmotic second virial coefficients, defined in a number density representation, that seem at least as universal as the product $[\eta]M$. This observation should *not* be extended to polymers in poor or Θ solvents or to charged polymers.

Acknowledgment. This work was supported by NSF Grants DMR-9634713 and DMR-0075810. The GPC/LS instrument was acquired through the Louisiana Board of Regents Trust Fund. We are grateful to William Daly and Javier Nakamatsu of this department for supplying many of the samples and to Dow Chemical for helpful advice on GPC.

References and Notes

- (1) Grubisic, Z.; Rempp, P.; Benoit, H. *J. Polym. Sci., Lett. Ed.* **1967**, *5*, 753–759.
- (2) Benoit, H. *J. Polym. Sci., Polym. Phys. Ed.* **1996**, *34*, 1703–1704.
- (3) Grubisic, Z.; Reibel, L.; Spach, G. *C. R. Acad. Sci. (Paris), Ser. C* **1967**, *264*, 1690–1693.
- (4) Casassa, E. F. *Macromolecules* **1976**, *9*, 182–185.
- (5) Elias, J. G.; Eden, D. *Macromolecules* **1981**, *14*, 410–419.
- (6) le Maire, M.; Viel, A.; Moller, J. V. *Anal. Biochem.* **1989**, *28*, 50–56.
- (7) Radic, D.; Gargallo, L.; Leon, A.; Horta, A. *J. Macromol. Sci., Phys.* **1992**, *B31*, 215–225.
- (8) Bahary, W. S.; Jilani, M. *J. Appl. Polym. Sci.* **1993**, *48*, 1531–1538.
- (9) Dubin, P. L.; Principi, J. M. *Macromolecules* **1989**, *22*, 1891–1896.
- (10) Dubin, P. L. *Adv. Chromatogr.* **1992**, *31*, 119–151.
- (11) Haney, M. A. *Am. Lab.* **1985**, *17*, 41–56.
- (12) Haney, M. A. *Am. Lab.* **1985**, *17*, 116–126.
- (13) Lecacheux, D.; Lescq, J. *J. Liq. Chromatogr.* **1982**, *5*, 2227–2239.
- (14) Deming, T. J.; Curtin, S. A. *J. Am. Chem. Soc.* **2000**, *122*, 5710–5717.
- (15) Deming, T. J. *Macromolecules* **1999**, *32*, 4500–4502.
- (16) Deming, T. J. *J. Am. Chem. Soc.* **1998**, *120*, 4240–4241.
- (17) Spatorico, A. L.; Coulter, B. *J. Polym. Sci., Polym. Phys. Ed.* **1973**, *11*, 1139–1150.
- (18) Poche', D. S.; Daly, W. H.; Russo, P. S. *Macromolecules* **1995**, *28*, 6745–6753.
- (19) Bu, Z.; Russo, P. S.; Tipton, D. L.; Negulescu, I. I. *Macromolecules* **1994**, *27*, 6871–6882.
- (20) Fujita, H.; Teramoto, A.; Yamashita, T.; Okita, K.; Ikeda, S. *Biopolymers* **1966**, *4*, 781–791.
- (21) Doty, P.; Bradbury, J. H.; Holtzer, A. M. *J. Am. Chem. Soc.* **1956**, *78*, 947–954.
- (22) Nakamatsu, J. Synthesis, Characterization, Liquid Crystals and Cross-linking of Poly(γ -alkyl- α -L-glutamates). Ph.D. Thesis, Louisiana State University. 1995.
- (23) Daly, W. H.; Poche', D. S. *Tetrahedron Lett.* **1988**, *29*, 5859–5862.
- (24) DeLong, L. M.; Russo, P. S. *Macromolecules* **1991**, *24*, 6139–6155.
- (25) Mächtle, W.; Fischer, H. *Angew. Makromol. Chem.* **1969**, *7*, 147–180. Huglin, M. B. In *Light Scattering from Polymer Solutions*; Huglin, M. B., Ed.; Academic Press: New York, 1972; pp 165–203.
- (26) Dawkins, J. V.; Hemming, M. *Polymer* **1975**, *16*, 554–560.
- (27) Tanford, C. *Physical Chemistry of Macromolecules*; John Wiley & Sons: New York, 1961; p 196.
- (28) Onsager, L. *Ann. N. Y. Acad. Sci.* **1949**, *51*, 627–659.
- (29) *Polymer Handbook*, 4th ed.; Brandrup, J., Immergut, E. H., Grulke, E. A., Eds.; Wiley: New York, 1999; Chapter VII, p 182, Table 16. Venkataswamy, K.; Jamieson, A. M.; Petshek, R. G. *Org. Coat. Appl. Polym. Sci. Proc.* **1986**, *55*, 339–344.
- (30) Yamakawa, H. *Modern Theory of Polymer Solutions*; Harper and Row: New York, 1971; Section 9.
- (31) Cotts, P. M.; Swager, T. M.; Zhou, Q. *Macromolecules* **1996**, *29*, 7323–7328.
- (32) Aharoni, S. M. *Macromolecules* **1983**, *16*, 1722–1728.
- (33) Yamakawa, H. *Annu. Rev. Phys. Chem.* **1984**, *35*, 23–47.
- (34) Schmidt, M. *Macromolecules* **1984**, *17*, 553–560.
- (35) Jamil, T.; Russo, P. S. *J. Chem. Phys.* **1992**, *97*, 2777–2782.
- (36) Kubota, K.; Tominaga, Y.; Fujime, S. *Macromolecules* **1986**, *19*, 1604–1612.
- (37) Russo, P. S.; Miller, W. G. *Macromolecules* **1984**, *17*, 1324–1331.

MA0013511